



Evaluation of the effective bulk composition (EBC) during growth of garnet

Frank S. Spear*, Oliver M. Wolfe

Department of Earth and Environmental Sciences, Rensselaer Polytechnic Institute, 110 8th Street, Troy, NY 12180, United States

ARTICLE INFO

Editor: K. Mezger

Keywords:

Garnet

Effective bulk composition

Nucleation and growth

Overstepping

ABSTRACT

The effective bulk composition (EBC) for the initial growth of garnet that has nucleated only after considerable overstepping of the equilibrium garnet-in reaction has been calculated for eight samples from central Vermont. The method developed assumes that the composition of garnet is determined by the maximum driving force (maximum change in Gibbs free energy) at the assumed conditions of nucleation. The method of intersecting isopleths is used to find the EBC where the isopleth intersection matches the P-T conditions of nucleation.

The calculated EBC for all samples (four epidote-free and four epidote-bearing) contains less MnO and FeO (or lower FeO/MgO) than the whole rock bulk composition. The CaO content of the EBC is lower than the whole rock bulk composition in all epidote-free samples and in two of the four epidote-bearing samples. It is proposed that the differences between the EBC and whole rock bulk composition are caused by the sluggish kinetics of dissolution of reactants rather than diffusive transport of nutrients to the garnet.

1. Introduction

The composition of garnet is assumed to reflect the P-T conditions and effective bulk composition as it grows, and numerous studies have utilized garnet composition to infer what those P-T conditions were and how they changed during growth. Some methods utilize only intensive thermodynamic parameters (i.e. P, T and composition) so knowledge of the effective bulk composition is not required; e.g. the Gibbs method (Spear and Selverstone, 1983) or inclusion thermometry and barometry (St-Onge, 1987). The limitation of these methods is that appropriate samples with sufficiently low variance or the necessary inclusion suites are rare. Other methods based on metamorphic assemblage diagrams (MADs or pseudosections) invoke mass balance constraints that require knowledge of the effective bulk composition from which garnet grows at every instant in time to produce meaningful results. A limitation of both these methods is the requirement that garnet grows in equilibrium with its surroundings, and a number of studies have concluded that, in fact, porphyroblasts nucleate and grow only after considerable overstepping (e.g. Hollister, 1969; Waters and Lovegrove, 2002; Pattison and Tinkham, 2009; Spear et al., 2014; Castro and Spear, 2016; Wolfe and Spear, 2018). In contrast, still other studies have assumed that the deviation from equilibrium is sufficiently small that equilibrium modeling provides a robust evaluation of the P-T conditions of garnet growth (e.g. George and Gaidies, 2017).

This paper presents an approach that provides constraints on the effective bulk composition (EBC) at the initiation of garnet growth after considerable overstepping. In the case where the P-T conditions of

garnet nucleation are independently known, and the composition of nucleated garnet follows the principle of maximum chemical driving force, the method of intersecting isopleths for the garnet core composition constrains the amounts of certain system components in the EBC. This approach reveals systematic gradients in Mn, Ca, Fe and Mg that indicate, in the cases examined, garnet is not growing in an EBC that corresponds to the bulk rock composition.

2. Theory

2.1. Method of intersecting isopleths

Duhem's theorem (Prigogine and Defay, 1954) states that for any system of any number of phases in which the bulk composition is known, there are only two degrees of freedom. This theorem forms the theoretical basis for the calculation of isochemical mineral assemblage diagrams (MADs or pseudosections). Thus, if the bulk composition is known, any two independent measured mineral compositions can be used to infer the pressure and temperature at the time the mineral obtained that composition, provided the mineral grows in equilibrium. Garnet contains three independent compositional parameters in its major components (e.g. almandine, spessartine, and grossular) and it has become common practice to use the method of intersecting isopleths to infer the conditions at which a particular garnet grew (e.g. Moynihan and Pattison, 2013; Gaidies et al., 2015; Dragovic et al., 2012; George and Gaidies, 2017, and references therein). Isopleths for all three independent components can be plotted with the expectation

* Corresponding author.

E-mail address: spear@rpi.edu (F.S. Spear).

that they will intersect at a point in P-T space. In many of the above cited papers, the intersection of these isopleths lie near, or slightly above, the calculated garnet isograd on a MAD for the bulk composition in question, leading to the reasonable conclusion that garnet nucleated at conditions just above the equilibrium isograd. Sophisticated models have been developed in which the bulk composition is continuously adjusted to account for fractionation of garnet so that an array of P-T points (the P-T path) can be inferred from the zoning preserved in garnet (Moynihan and Pattison, 2013; George and Gaidies, 2017, and references therein). All of these applications assume equilibrium between the growing garnet and the effective bulk composition.

2.2. Method of maximum driving force

Recent studies, however, in which quartz-inclusion-in-garnet (QuiG) barometry has been used to infer the pressure at which garnet nucleated (e.g. Spear et al., 2014; Castro and Spear, 2016; Wolfe and Spear, 2018) conclude that garnet nucleates at pressures and temperatures considerably above the conditions inferred from intersecting garnet core isopleths, leading to the conclusion that considerable overstepping is required for garnet to nucleate. Furthermore, Spear et al. (2014) present a method for calculating the composition of garnet that nucleates after any degree of overstepping and demonstrate that, if this composition is used assuming nucleation under equilibrium conditions, then the intersecting isopleth method returns P-T conditions that typically fall just above the equilibrium garnet isograd. Thus, the inference that the garnet nucleated very nearly on the equilibrium isograd based on the intersecting isopleths may be spurious and should be carefully evaluated. For example, the study of George and Gaidies (2017) has shown that the difference in P-T conditions between the calculated garnet isograd and those inferred from intersecting isopleths of the garnet core is within the uncertainty of the thermochemical data thus making it difficult to draw a definitive conclusion about the degree of overstepping without an independent means of determining the P-T conditions of garnet nucleation.

The method presented by Spear et al. (2014) is based on an approach described by Thompson and Spaepen (1983) and discussed by Pattison et al. (2011). Briefly, the method assumes that the composition of garnet that forms at any overstepped P-T conditions is that which will result in the greatest decrease in Gibbs free energy (G), which Thompson and Spaepen (1983) and Hillert (2008) equate with the maximum driving force for nucleation or growth. This can be shown graphically for a pseudobinary system as the free energy difference between the tangent plane for the matrix assemblage and the parallel tangent plane to the garnet free energy surface (e.g. Fig. 1 of Spear et al., 2014 and Fig. 1 of Spear, 2017). This method is herein termed the “overstep model” or OS model and was used by Pattison et al. (2011), Gaidies et al. (2011), Spear et al. (2014), Castro and Spear (2016) and Wolfe and Spear (2018) to calculate the composition of garnet at the point of nucleation and by Spear (2017) to calculate the entire isothermal, isobaric growth zoning of garnet.

The method of maximum driving force provides a means to calculate the composition of any phase that is out of equilibrium with the assemblage from which it is nucleating or growing. If the overstepped P-T conditions at which a natural garnet nucleates are known, then it follows that the method of intersecting isopleths using this OS model should recover those P-T conditions when applied to the measured garnet and bulk composition. As will be presented below in the results section, this turns out not to be the case. When the OS model is used with the method of intersecting isopleths for garnets with well-constrained P-T conditions of nucleation and growth, the isopleths intersect at conditions that are geologically unreasonable, typically at much higher pressures and temperatures than are possible. One possible explanation of this discrepancy is that the OS model of maximal driving

force is not correct. Inasmuch as this model is in wide use in the material sciences and has been demonstrated to reproduce experimental results involving crystal nucleation rates (e.g. Thompson and Spaepen, 1983, and references therein), it is not suspected that the model is grossly in error.

An alternative explanation is that the bulk composition used for calculation of the OS model is not the effective bulk composition that the garnet experiences as it grows. As illustrated in Fig. 1a, the composition of garnet grown under equilibrium conditions is independent of the bulk composition (within limits) in this pseudobinary projection. In contrast, examination of Fig. 1b reveals that the composition of garnet predicted by the OS model is highly sensitive to the EBC. Garnet bearing schists are not pseudobinary systems so variations in bulk rock composition will affect garnet composition in equilibrium calculations as, for example variations in the bulk MnO composition will affect the spessartine content of garnet. For the purposes of this study, the OS model calculation can serve as a sensitive monitor of the effective bulk composition during garnet growth.

2.3. Calculation of effective bulk composition (EBC)

The composition of garnet calculated with the OS model is a function of the P-T conditions, the assemblage from which garnet nucleates and grows (the paleoassemblage), and the effective bulk composition. If the P, T, and paleoassemblage are known, then select elements in the EBC can be calculated such that the garnet compositional isopleths intersect at exactly the known P-T conditions.

There are only three independent garnet compositional isopleths so there are three independent equations that can be used. Choosing almandine, spessartine and grossular as the independent components in garnet, the equations to solve are

$$0 = (X_{\text{alm,Meas}} - X_{\text{alm,Calc}})$$

$$0 = (X_{\text{sps,Meas}} - X_{\text{sps,Calc}})$$

$$0 = (X_{\text{grs,Meas}} - X_{\text{grs,Calc}})$$

where $X_{\text{alm,Meas}}$ and $X_{\text{alm,Calc}}$ are the measured and calculated (from the OS model) almandine values. Inasmuch as there are only three independent equations, only three system components can be solved for at a time. For example, solving for FeO, MnO, and CaO in the EBC and utilizing Newton's method for the solution, these equations can be written as:

$$0 = (X_{\text{alm,Meas}} - X_{\text{alm,Calc}}) + \left(\frac{\partial X_{\text{alm}}}{\partial \text{Fe}} \right)_{\text{Mn,Ca}} \Delta \text{Fe} + \left(\frac{\partial X_{\text{alm}}}{\partial \text{Mn}} \right)_{\text{Fe,Ca}} \Delta \text{Mn} + \left(\frac{\partial X_{\text{alm}}}{\partial \text{Ca}} \right)_{\text{Fe,Mn}} \Delta \text{Ca}$$

$$0 = (X_{\text{sps,Meas}} - X_{\text{sps,Calc}}) + \left(\frac{\partial X_{\text{sps}}}{\partial \text{Fe}} \right)_{\text{Mn,Ca}} \Delta \text{Fe} + \left(\frac{\partial X_{\text{sps}}}{\partial \text{Mn}} \right)_{\text{Fe,Ca}} \Delta \text{Mn} + \left(\frac{\partial X_{\text{sps}}}{\partial \text{Ca}} \right)_{\text{Fe,Mn}} \Delta \text{Ca}$$

$$0 = (X_{\text{grs,Meas}} - X_{\text{grs,Calc}}) + \left(\frac{\partial X_{\text{grs}}}{\partial \text{Fe}} \right)_{\text{Mn,Ca}} \Delta \text{Fe} + \left(\frac{\partial X_{\text{grs}}}{\partial \text{Mn}} \right)_{\text{Fe,Ca}} \Delta \text{Mn} + \left(\frac{\partial X_{\text{grs}}}{\partial \text{Ca}} \right)_{\text{Fe,Mn}} \Delta \text{Ca}$$

where Fe, Mn and Ca are used to refer to FeO, MnO, and CaO. The computational algorithm is as follows:

1. Pick a bulk composition — this is typically the measured whole rock bulk composition

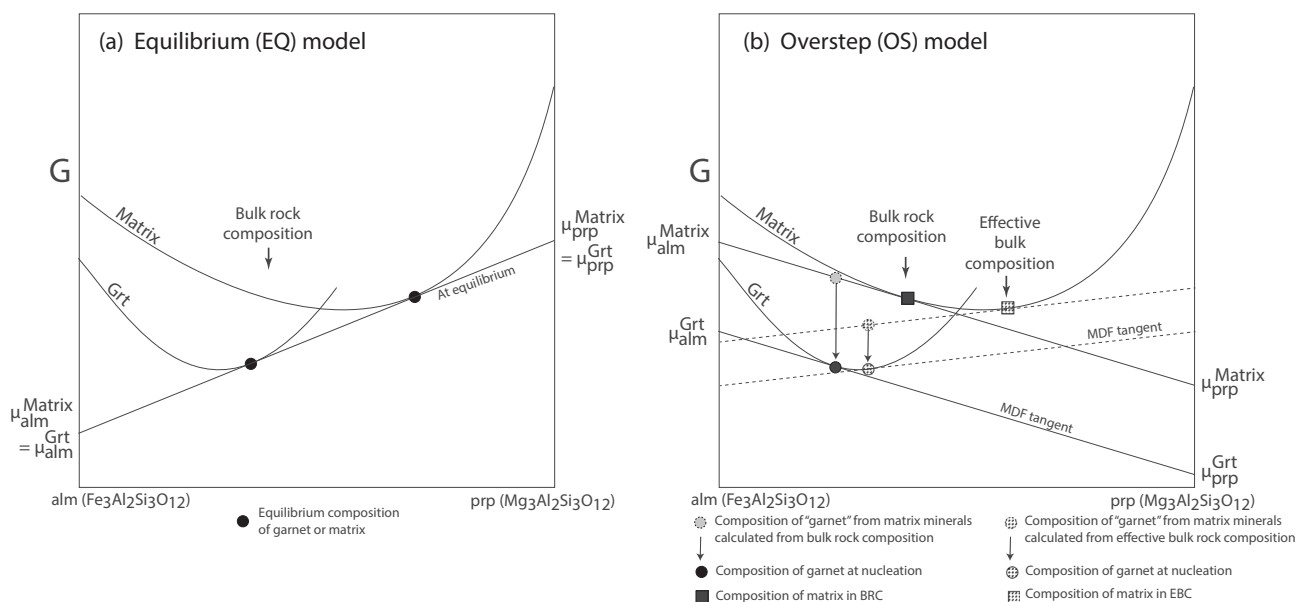


Fig. 1. Schematic binary G-X diagrams. (a) The equilibrium (EQ) model. Note that the compositions of both garnet and matrix phases are insensitive to changes in the bulk rock composition. (b) Overstep (OS) model. Solid lines and symbols show the composition of garnet that would nucleate from the bulk rock composition. Dashed lines and dotted symbols show the composition of garnet that would nucleate from the effective bulk composition. MDF tangent is the tangent from the maximum driving force model.

2. Pick a paleoassemblage from which garnet nucleates or grows.
3. Calculate the compositions and amounts of phases in the paleoassemblage at the presumed P-T conditions of garnet nucleation or growth using the EBC. In the initial step the EBC is the same as the original whole rock bulk composition (the OBC). Note that this step assumes that the paleoassemblage is in equilibrium with the EBC.
4. Calculate the composition of garnet that would form from this assemblage and the assumed P-T conditions using the OS model.
5. Compare the measured and calculated garnet compositions to see if they match. If they do match, then the problem is done.
6. If the compositions do not match, calculate the derivatives in the above equations using a finite difference approximation.
7. Solve for ΔFeO , ΔMnO , ΔCaO and recalculate the EBC.
8. Go to 3 and continue to iterate until convergence.

Because there are only three system components that may be solved for at a time, the other system components must be held constant for the algorithm to work. The choice of system components to hold constant and which ones to manipulate will be discussed in the results section below.

2.4. Calculation of P-T conditions for garnet nucleation and growth

The goal of this study is to place constraints on the EBC during growth of the garnet core. It is important to note that it is not assumed that the measured composition of the garnet core is the same as the composition of the initial garnet nucleus. Indeed, if the nucleus was of a composition significantly different from the growing core then diffusion would surely have erased this compositional difference due to the small size of the nucleus. The critical assumption to these calculations is that the maximum driving force calculation described above can also be applied to subsequent growth of the garnet as was done by Spear (2017). Critical to the calculation is independent assessment of the P-T conditions of garnet nucleation and growth of the core.

The method for determining the conditions at which garnet nucleates and grows must not involve assumptions about the EBC (i.e. use of MADs) because the EBC is assumed to be unknown in this procedure. The method used here is adopted from the approach developed by

Wolfe and Spear (2018). Pressure is estimated from application of quartz-inclusion-in-garnet (QuiG) barometry (Kohn, 2014; Spear et al., 2014). The experimental study of Thomas and Spear (2018) confirms that QuiG barometry is capable of reproducing experimental pressures of garnet growth to better than 10%, which for our samples indicates that the QuiG pressures are accurate to within around ± 1 kb. Temperature is somewhat more difficult to constrain because applicable thermometers require assumptions about chemical equilibrium, and it is known from application of QuiG barometry that garnet nucleates only after considerable overstepping of the equilibrium isograd reaction.

Several of the samples examined for this study contain garnet with ilmenite inclusions in the core and rutile inclusions approximately half way towards the garnet rim. This texture has been interpreted (Wolfe and Spear, 2018) as indicating that the reaction of ilmenite to rutile has been crossed during the growth of garnet. Results for sample TM-921 (see Wolfe and Spear, 2018, for sample locations) are shown in Fig. 2. The equilibrium MAD (Fig. 2a) has been calculated for the measured bulk composition with the suppression of rutile nucleation to illustrate the degree of overstepping of garnet nucleation (black square). The bulk composition was then fractionated based on integrating a series of spherical shells using the measured zoning profile up to the point where rutile is observed as inclusions in garnet and a second MAD calculated (Fig. 2b). The rutile isograd occurs at close to 8.5 kb, which is below the pressure of garnet nucleation and consistent with the formation of rutile during growth of garnet. Hence, the phase equilibria calculations (Fig. 2) are in accord with the observed textural relations.

The calculations illustrated in Fig. 2 support the textural interpretation that rutile nucleated and grew while garnet was growing. Therefore, we can safely conclude that thermometry using zirconium in rutile (ZiR; Tomkins et al., 2007) will accurately reflect the temperature at one point during garnet growth to an uncertainty of approximately $\pm 15^\circ$ (Tomkins et al., 2007), provided that equilibrium among rutile, zircon and quartz was attained. It will be assumed that this temperature reflects the temperature during the entire duration of garnet growth (i.e. garnet growth was isothermal and isobaric). Whereas it is entirely possible that P and T changed during garnet growth, the following observation suggests that such changes were not substantial. Measurement of quartz inclusion Raman shifts show no

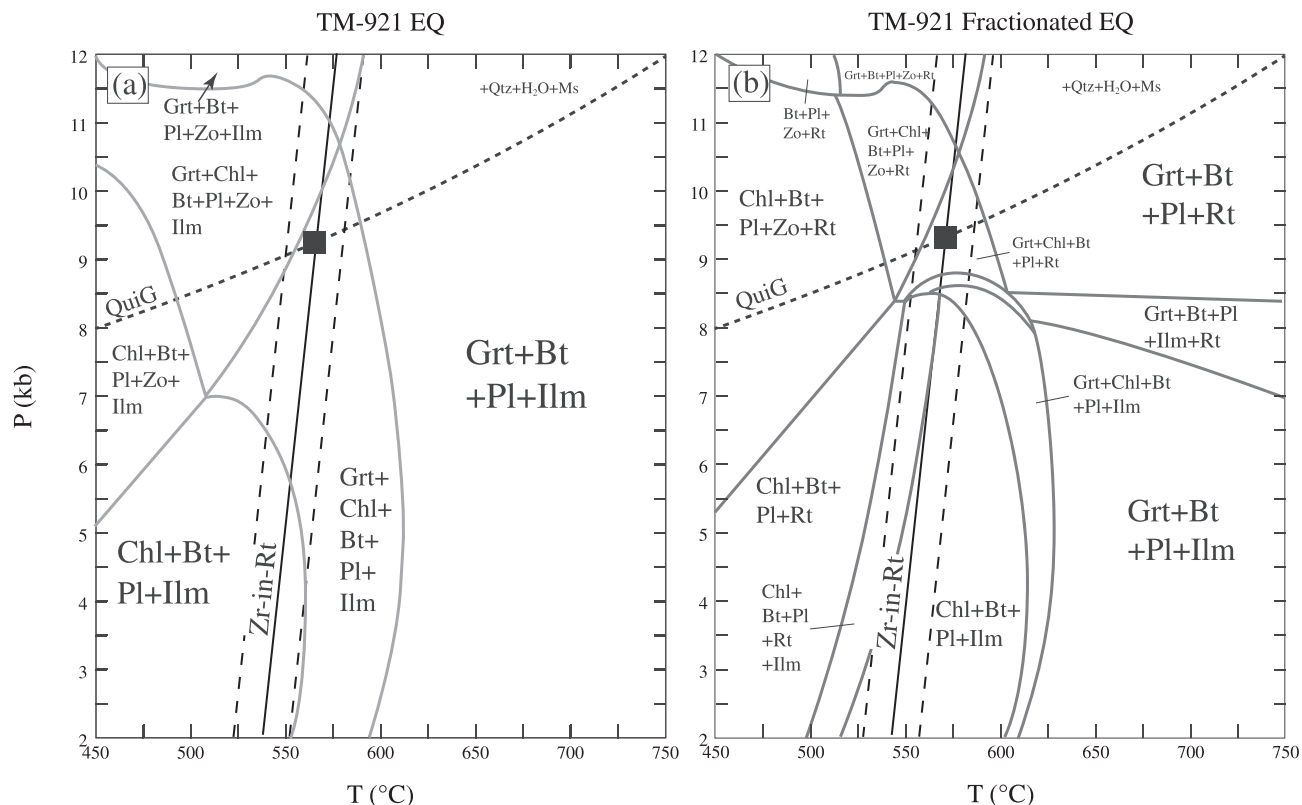


Fig. 2. Isochemical MADs showing distribution of assemblages in P-T space for sample TM-921 calculated using the SPaC thermodynamic dataset (Spear and Pyle, 2010). (a) Equilibrium MAD using the measured bulk composition. (b) Equilibrium MAD using the bulk composition fractionated by removing garnet up to the point where rutile enters the assemblage. Note that the rutile-in isograd, which does not appear at all in (a) moves to lower pressure and plots below the QuiG isograds (dashed lines). Results from the zirconium-in-rutile thermometer (Tomkins et al., 2007) are shown with 1 sigma uncertainties. The inferred conditions of garnet nucleation are shown in each diagram as a square (see also Table 2).

pattern with respect to position within garnet (see Wolfe and Spear, 2018, for details). Therefore, if P and T did change during garnet growth they must have changed in concert such that they followed the QuiG isograds, which has a slope of around $20^{\circ}/\text{km}$. A P-T path with such a shallow slope is inconsistent with the metamorphism being driven by active tectonic loading (i.e. the P-T paths would be much steeper), so we adopt the limiting conclusion that garnet growth was very nearly isothermal and isobaric. In any event, this study is focused on the composition of the garnet core so the P-T path during the majority of garnet growth is immaterial. Most importantly for the present study, we assume that the P-T conditions of the garnet core are those obtained from the intersection of QuiG and ZiR. For sample TM-921 these conditions are 570°C , 9.4 kb (Table 2). In samples that do not contain rutile inclusions within garnet, the temperature of nucleation has been arbitrarily set at 575°C except for sample OW-5C for which thermobarometry indicates a peak temperature of 560°C (Menard and Spear, 1994). The impact of changing the assumed temperature of nucleation on the calculated results are discussed below.

3. Results

Eight samples from the Connecticut Valley synclinorium in central Vermont and western Massachusetts were chosen for study. Four samples are epidote-free and four are epidote-bearing at the time of garnet nucleation. These samples were chosen because of the simple and well-characterized metamorphic history (e.g. Menard and Spear, 1994; Wolfe and Spear, 2018) and because they contain the appropriate assemblages and garnet inclusion suites for accurate determination of the P-T conditions of garnet nucleation. Sample locations, mineral assemblages, and inferred paleoassemblages are given in Table 1. The

compositions of the garnet cores are presented in Table 2. More detailed descriptions of the textures and microstructures for several samples are presented in Wolfe and Spear (2018).

To place the results of this study in context, MADs were calculated from the bulk compositions listed in Tables 4 and 5 for each of the eight samples to determine the location of the garnet isograd and isopleths for almandine, spessartine, and grossular plotted (Fig. 3). Calculations were performed using both the SPaC dataset (Spear and Pyle, 2010) and the Thermocalc dataset ds6.2 (HP11) (Holland and Powell, 2011; White et al., 2014a, 2014b). The four epidote-free samples (OW-19, TM-626, TM-916c, and TM-918c) all show similar characteristics. In each case, the intersecting isopleths plot above the garnet isograd calculated with both the SPaC and HP11 datasets. It should be noted that for all samples studied, the garnet isograd calculated from the HP11 dataset plotted below 450°C , which seems to be much too low based on other phase equilibria constraints. The intersecting isopleths also plot below the pressure determined for garnet nucleation based on application of QuiG. Epidote-bearing samples show more variable behavior. As with the epidote-free samples, the intersecting isopleths all plot above the equilibrium garnet isograd determined from either the SPaC or HP11 datasets. Again, the isograds calculated from the HP11 dataset plot at unreasonably low temperatures for these samples. Three epidote-bearing samples were studied in detail by Wolfe and Spear (2018). Intersecting isopleths for these samples from that study plot at lower pressures than those calculated in the present study. In Wolfe and Spear (2018), all iron was assumed to be FeO and the epidote phase was modeled as pure clinozoisite whereas in the present study, 0.5 wt% was assumed to be Fe₂O₃ and epidote was modeled as a binary clinozoisite-pistacite solution. Although this assumption regarding ferric iron displaced the equilibrium isopleths, in some cases considerably (e.g.

Table 1
Samples, location and assemblages.

Sample	Latitude ^a	Longitude ^a	Formation name	Mapped grade	Minerals present	Garnet inclusion suite	Observed paleo assemblage
TM-916c	43.82365	-72.54980	Gile mountain	Grt	Qtz-Ms-Pl-Bt-Grt-Ilm-Chl-Ep-Aln-Py-Ap-Cal-Tur-Gr	Qtz-Ap-Ilm-Py	Qtz + Ms + Pl + Bt + Chl + Ilm + Ap + Zrn + Py + Gr
TM-918C	43.85022	-72.54277	Waits river	Grt	Qtz-Ms-Pl-Bt-Grt-Ilm-Chl-Py-Ap-Zrn-Tur-Gr	Qtz-Ap-Ilm-Py-Zr	Qtz + Ms + Pl + Bt + Chl + Ilm + Ap + Zrn + Py + Gr
TM-921	43.81378	-72.50533	Waits river	St-Ky	Qtz-Ms-Pl-Bt-Grt-Fp-St-Aln-Chl-Rt-Ilm-Py-Po-Ap-Xen-Zrn-Gr	Qtz-Rt-Ilm-Ep-Aln-Py-Ap-Zrn	Qtz + Ms + Pl + Bt + Chl + Zo + Rt + Ilm + Ap + Zrn + Py + Gr
TM-675	43.80940	-72.50371	Waits river	St-Ky	Qtz-Ms-Pl-Bt-Grt-Ep-Ilm-Chl-Rt-Ap-Zrn-MnZ-Tur-Gr	Qtz-Ap-Rt	Qtz + Ms + Pl + Bt + Chl + Zo + Aln + Ap + MnZ + Zrn + Py + Gr
TM-678	43.79084	-72.46447	Gile mountain	St-Ky	Qtz-Ms-Pl-Bt-Grt-Ilm-Chl-Rt-Ap-Zrn-Tur-Ep-Gr	Qtz-Ms-Br-Pl-Fp-Rt-Ilm	Qtz + Ms + Pl + Bt + Chl + Zo + Rt + Ilm + Ap + Zrn + Py + Gr
OW-5C	43.82549	-72.62492	Moretown	Grt	Qtz-Ms-Pl-Bt-Grt-Ilm-Chl-Py-Ap-Zrn-Tur-Ep	Qtz-Pl-Ep-Tur-Ap-Ilm	Qtz + Ms + Pl + Bt + Chl + Zo + Aln + Ilm + Ap + Zrn + Py
TM-626 ^b	43.80450	-72.33500	Gile MOUNTAIN	St-Ky	Qtz-Ms-Pl-Bt-Grt-St-Chl-Rt-Ilm-Tur-Gr	Qtz-Ilm	Qtz + Ms + Pl + Bt + Chl + Gr
OW-19	42.45414	-72.88191	Goshen	St-Ky	Qtz-Ms-Pl-Bt-Grt-Ilm-Chl-Ap-Zrn-Gr-Rt	Qtz-Rt-Ilm-Ap	Qtz + Ms + Pl + Bt + Chl + Gr

^a Sample locations are accurate to approximately 10 m.

^b Sample data from Spear et al. (2014).

^c Kretz abb. not available: Xenotime, Xen;

sample TM-678), it does not greatly affect the calculation of the effective bulk composition (see below).

Table 3 shows detailed results of the EBC calculations for sample TM-626 (this and all subsequent calculations were done using the SPaC dataset). As mentioned above, inasmuch as there are only three independent components in garnet, only three system components can be modified at any one time and this table explores the effect of choice of system components to modify. Column 1 provides the whole rock analysis and each subsequent column provides the solution for different choices of system components. It was discovered that there are numerous choices of system components for which there is no solution (DNC = did not converge). For example, solutions in which K₂O, H₂O, SiO₂ or Al₂O₃ were chosen to modify (columns 5–8) did not converge. Examination of columns 2–4 reveals that solutions can be obtained with the choice of system components as FeO + MnO + CaO, MgO + MnO + CaO, FeO + MnO + Na₂O (presumably MgO + MnO + Na₂O would also work but this was not tried). Of course, the “true” effective bulk composition might, in fact, be some linear combination of all of the system components, but this is impossible to constrain mathematically. Nevertheless, there are systematics to the solutions that display commonalities. In all cases where FeO, MnO, and CaO were varied, the EBC value for these system components is lower than that of the original bulk composition (OBC). Allowing MgO to vary while holding FeO constant or Na₂O to vary while holding CaO constant results, as expected, in an increase of MgO or Na₂O relative to the OBC. It is reasonable to conclude, therefore, that the EBC for initial garnet growth reflects a lower Fe/Mg and a lower Ca/Na than the OBC. The MnO content of the EBC is always lower than that of the OBC.

Table 4 shows the results of EBC calculations for all epidote-free samples in which FeO, MnO and CaO were chosen as the system components to modify. The first three columns are all for sample TM-626 calculated for different pressures and temperatures from the nominal value of 575 °C, 10750 bars. As can be seen by examination of columns 1–3, the effect of changing T by 15 °C and P by 1 kb has little effect on MnO, a small effect on FeO, and a somewhat larger effect on CaO. Nevertheless, all values show the same directional change relative to the OBC for every temperature. The other four samples (columns 4–7) all show the same systematic changes as does TM-626.

Table 5 shows the results of similar calculations for samples that contain epidote. A number of calculations were performed in which it was assumed that the epidote-like mineral was pure clinozoisite (following Wolfe and Spear, 2018). It was found that no convergence was possible with clinozoisite in the paleoassemblage. This creates an additional uncertainty because in order to add epidote to the assemblage it was necessary to infer the Fe₂O₃ content of the OBC, which was not measured. A value of Fe₂O₃ = 0.5 wt% was adopted for all samples with FeO adjusted accordingly and columns 1 and 2 of **Table 5** explore the effect of varying Fe₂O₃ between 0.5 and 1.0 wt% for sample TM-675. As can be seen, the Fe₂O₃ content makes virtually no difference in the calculated MnO content of the EBC, a small difference in the calculated FeO content, but a significant difference in the calculated CaO content of the EBC. Specifically, as the Fe₂O₃ content increases, the difference between the EBC and OBC CaO content gets progressively less negative (CaO in the EBC is lower than that of the OBC) and would eventually go positive (CaO in the EBC is higher than that of the OBC) with sufficiently high Fe₂O₃ content. It must be concluded that this uncertainty in the Fe₂O₃ content of the OBC adds a degree of uncertainty to the discussion that follows.

Comparison of columns 1, 3 and 4 of **Table 5** reveal the effect of changing the P and T of garnet growth on the calculations for sample TM-675, keeping the Fe₂O₃ content constant at 0.5 wt%. As can be seen, the effect on MnO is negligible, the effect on FeO small, and the effect on CaO is significant with the difference in CaO between the EBC and OBC becoming less negative as T is increased and P is decreased. Results for the other three samples (columns 5, 6, 7 of **Table 5**) with Fe₂O₃ = 0.5 wt% all consistently show FeO and MnO to decrease in the

Table 2

Composition of garnet cores (wt% oxides).

Sample	Epidote-free samples				Epidote-bearing samples			
	OW-19	TM-626	TM-916C	TM-918C	TM-675	TM-678	TM-921	OW-5C
SiO ₂	36.45	36.62	34.75	37.97	37.53	37.85	36.25	37.11
TiO ₂	0.08	0.05	0.11	0.13	0.12	0.10	0.11	0.10
Al ₂ O ₃	21.08	21.55	21.48	21.21	21.17	21.2	21.45	21.02
FeO	29.78	29.10	30.81	26.38	25.14	25.13	27.88	27.94
MnO	4.30	8.82	3.57	6.20	5.60	7.12	4.11	7.08
MgO	1.07	1.65	1.17	1.54	1.72	1.33	1.82	1.26
CaO	6.62	3.30	7.20	7.63	8.06	8.25	8.6	6.77
Total	99.44	101.09	99.09	101.06	99.34	100.98	100.26	101.28
Pyp	0.043	0.066	0.045	0.061	0.069	0.052	0.070	0.049
Alm	0.669	0.645	0.674	0.589	0.569	0.555	0.602	0.607
Sps	0.098	0.193	0.079	0.141	0.128	0.159	0.090	0.156
Grs	0.190	0.096	0.202	0.209	0.234	0.234	0.238	0.188
Fe/Fe + Mg	0.940	0.907	0.937	0.906	0.892	0.914	0.896	0.925
T(°C)	575	575	575	575	560	565	570	560
P(kb)	10,000	10,750	9900	10,000	9500	8800	9400	8500

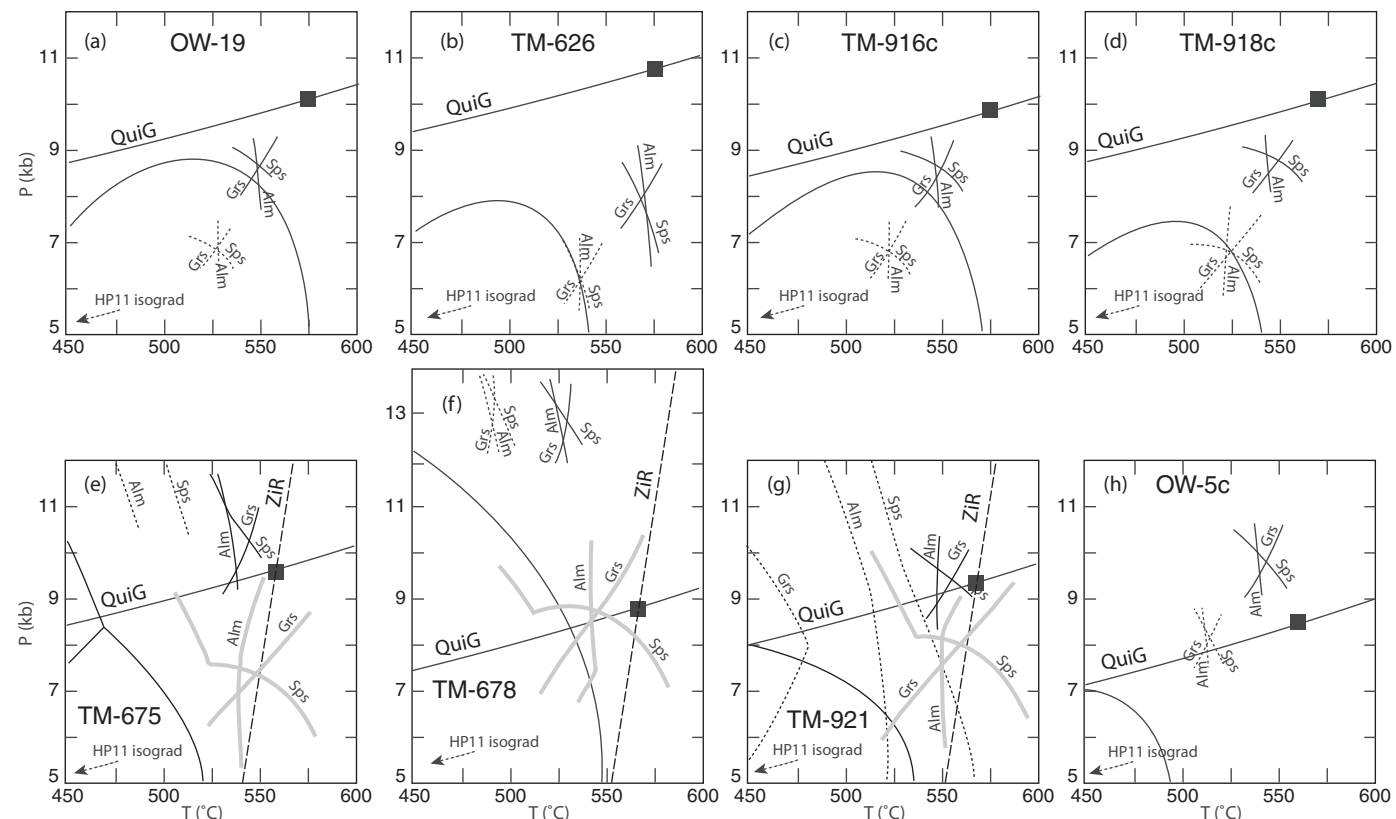


Fig. 3. Equilibrium garnet isograds and isopleths calculated for each sample using the SPaC (solid lines) and HP11-ds2.5 (dashed lines) data sets. Results of quartz-in-garnet barometry are labeled “QuiG”. Garnet core isopleths are labeled “Alm”, “Sps”, and “Grs” for calculations from each dataset. For samples TM-675, TM-678, and TM-921 (e, f, and g), the isopleths are calculated with epidote in the paleoassemblage assuming $\text{Fe}_2\text{O}_3 = 0.5$ wt%. Grey isopleths are from Wolfe and Spear (2018) assuming clinzozoisite rather than epidote in the paleoassemblage. Long dashes are the results of Zr-in-rutile (ZrR) thermometry from Wolfe and Spear (2018). Black boxes denote P-T conditions of calculations. Note that the garnet isograds calculated with the HP11-ds2.5 dataset plots at temperatures below 450 °C and thus do not appear on the diagram.

EBC whereas CaO decreases in sample TM-921 (column 5) but increases in samples TM-678 (column 6) and OW-5c (column 7).

4. Discussion

The results shown in Tables 4 and 5 are consistent with the interpretation that the EBC experienced by garnet during initial growth is lower in FeO (or higher in MgO or both) and lower in MnO than the OBC, irrespective of whether epidote is present. The results for CaO are

more difficult to generalize, but it appears that CaO in the EBC for epidote-free samples is always lower than in the OBC. For epidote-bearing samples, the uncertainties in the bulk rock Fe_2O_3 renders the results too uncertain to draw definitive conclusions, with some samples showing CaO in the EBC to be higher than in the OBC whereas in others it is lower.

To further understand the relationship between calculations assuming equilibrium (the EQ model) and calculations using the maximum driving force model (the MDF or OS model), Table 6 has been

Table 3

Variation of EBC with choice of independent system components for sample TM-626 (wt% oxides).

	1	2	3	4	5	6	7	8
	OBC	EBC	EBC	EBC	EBC	EBC	EBC	EBC
SiO ₂	55.72							xx
Al ₂ O ₃	16.16						xx	
MgO	3.97		5.60					
FeO	10.76	7.52		7.88	xx			
MnO	0.44	0.16	0.22	0.14	xx	xx	xx	
CaO	0.64	0.23	0.23		xx	xx	xx	
Na ₂ O	1.25			3.54				
K ₂ O	4.05				xx			
H ₂ O	6.00					xx		
					DNC	DNC	DNC	DNC

OBC = original bulk composition.

EBC = effective bulk composition.

DNC = did not converge.

Table 4

Calculated EBC for epidote-free samples (wt% oxides)^a.

	1	2	3	4	5	6
T(°C)	575	560	575	575	575	575
P(kb)	10,750	10,750	9750	9900	10,000	10,000
	TM-626	TM-626	TM-626	TM-916c	TM-918c	OW-19
SiO ₂	55.72	55.72	55.72	62.19	71.58	72.12
Al ₂ O ₃	16.16	16.16	16.16	21.03	13.49	12.87
MgO	3.97	3.97	3.97	1.48	1.59	1.28
FeO	10.76	10.76	10.76	5.45	4.88	4.58
MnO	0.44	0.44	0.44	0.06	0.17	0.05
CaO	0.64	0.64	0.64	0.74	1.71	0.72
Na ₂ O	1.25	1.25	1.25	1.03	2.55	1.15
K ₂ O	4.05	4.05	4.05	5.72	2.06	3.37
H ₂ O	10.00	10.00	10.00	10.00	10.00	10.00
Effective bulk composition ^b						
FeO	7.52	7.15	7.62	3.53	2.65	3.43
MnO	0.16	0.14	0.16	0.03	0.04	0.03
CaO	0.23	0.16	0.31	0.71	1.58	0.72
Difference						
FeO	-3.24	-3.61	-3.14	-1.92	-2.23	-1.15
MnO	-0.28	-0.30	-0.28	-0.03	-0.13	-0.02
CaO	-0.41	-0.48	-0.33	-0.03	-0.13	0.00

^a Bulk compositions were determined from integration of scans using the electron microprobe of thin sections.

^b Effective bulk composition calculated for selected elements as described in the text.

created to compare both the observed and calculated compositions of the garnet core as well as the measured bulk rock composition (OBC) and the effective bulk rock composition calculated assuming both of these models for sample TM-626. As can be seen from Table 6, the calculated garnet core compositions are quite different depending on whether equilibrium or overstepping is assumed. Notably, the spessartine content is 0.104 and 0.307 for the EQ and OS models, respectively, whereas the measured value of 0.193 lies in between. Thus, the EBC necessary to obtain the measured value of $X_{\text{sp}} = 0.193$ is quite different depending on whether equilibrium or overstepping is assumed to control garnet growth. In particular, the OS model predicts an EBC with MnO = 0.16 wt% whereas the EQ model predicts an EBC with MnO = 1.16 wt%, as compared with the measured MnO content (OBC) of 0.44 wt%. Although there is no way to independently verify which, if either, of these calculations of the EBC is correct, it does not seem likely that the EBC in the vicinity of a growing garnet would be enriched in MnO relative to the OBC. Thus it is concluded that the equilibrium calculation is not an appropriate calculation of garnet composition for a crystal that is so far out of equilibrium. It should be reemphasized that

Table 5

Calculated EBC for epidote-bearing samples (wt% oxides)^a.

	1	2	3	4	5	6	7
T(°C)	560	560	560	575	570	565	560
P(kb)	9500	9500	10,500	9500	9400	8800	8500
	TM-675	TM-675	TM-675	TM-675	TM-921	TM-678	OW-5C
SiO ₂	50.09	50.09	50.09	50.09	52.41	72.94	49.15
Al ₂ O ₃	22.96	22.96	22.96	22.96	22.26	10.88	24.04
Fe ₂ O ₃	0.50	1.00	0.50	0.50	0.50	0.50	0.50
MgO	2.10	2.10	2.10	2.10	1.96	1.80	1.60
FeO	6.66	6.66	6.66	6.66	5.72	4.59	5.65
MnO	0.31	0.31	0.31	0.31	0.21	0.18	0.36
CaO	3.06	3.06	3.06	3.06	3.16	1.20	2.18
Na ₂ O	2.29	2.29	2.29	2.29	2.69	1.89	3.31
K ₂ O	4.17	4.17	4.17	4.17	3.97	2.08	4.58
H ₂ O	10.00	10.00	10.00	10.00	10.00	10.00	10.00
Effective bulk composition ^b							
FeO	2.51	2.56	2.47	2.75	2.64	3.51	3.33
MnO	0.04	0.04	0.04	0.04	0.03	0.05	0.05
CaO	2.08	2.98	1.72	2.91	2.92	3.00	3.25
Difference							
FeO	-4.15	-3.54	-4.19	-3.91	-3.08	-1.08	-2.32
MnO	-0.27	-0.27	-0.27	-0.27	-0.18	-0.13	-0.31
CaO	-0.98	-0.08	-1.34	-0.15	-0.24	1.80	1.07

^a Bulk compositions were determined from integration of scans using the electron microprobe of thin sections.

^b Effective bulk composition calculated for selected elements as described in the text.

Table 6

Comparison of garnet core composition and effective bulk composition assuming equilibrium (EQ model) and overstepping (OS model) for sample TM-626.

	Garnet core composition		
	Measured	Calc-EQ ^a	Calc-OS ^a
Prp	0.066	0.062	0.036
Alm	0.645	0.709	0.505
Sps	0.193	0.104	0.307
Grs	0.096	0.125	0.152
	Amounts of selected system components		
	OBC ^b	EBC ^c -EQ model ^a	EBC ^c -OS model ^a
FeO	10.76	11.76	7.52
MnO	0.44	1.16	0.16
CaO	0.64	0.74	0.23

^a Calculated at the conditions garnet core growth inferred from the intersection of QuiG and ZiR ($T = 575$ °C, $P = 10,750$ bars).

^b OBC = original (measured) bulk composition.

^c EBC = effective (calculated) bulk composition.

the intersecting isopleths for the garnet core for sample TM-626 (Fig. 3b) fall approximately 2.75 kb below the pressure established by QuiG barometry but only 25–30° above the equilibrium garnet isograd. Thus, if these equilibrium isopleth intersections were used to infer the conditions of garnet core growth, it would be concluded that there was around 25–30° of overstepping. However, the independent determination of the pressure of garnet core formation conditions from QuiG reveal amount of overstepping to be around 50 °C and 3 kb. It must be concluded that the intersecting isopleth method, when applied using equilibrium calculations to crystals that are growing after considerable overstepping, are likely to yield spurious results. It should also be noted that this comparison is only possible because an independent estimate of the P-T conditions of garnet core growth are available through the use of QuiG barometry and, for some samples, ZiR thermometry. Attempts to establish whether garnet grows close to, or far from, equilibrium by using only equilibrium calculations are circular, at best.

Two possible explanations for the difference between the EBC and

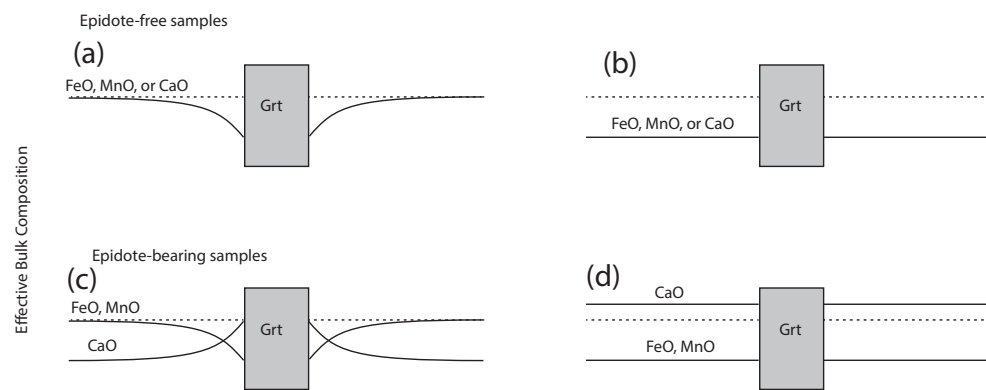


Fig. 4. Cartoon showing two possible explanations for the difference between the measured bulk composition (OBC – dashed lines) and the effective bulk composition (EBC – solid lines) for epidote-free samples (a and b) and epidote-bearing samples (c and d). (a) and (c) show the EBC as a function of limited diffusion through grain boundaries. (b) and (d) show the EBC as a function of equilibria between matrix minerals and the grain boundary, presumably as a result of kinetically limited dissolution of reactants.

OBC are examined in Fig. 4. In Fig. 4a and c the EBC is depicted as resulting from diffusional gradients in the rock matrix. In Fig. 4b and d the EBC is depicted as homogeneous in the matrix (i.e. no diffusional gradients), in which case the EBC must be controlled by another mechanism that involves the matrix phases. Possibilities include (a) partitioning between matrix phases and the grain boundary medium; (b) sluggish diffusion of nutrients from within matrix phases into the grain boundary medium; (c) sluggish dissolution of matrix phases that contain essential components. Although it is not possible at this time to unequivocally distinguish between these two models, there are two reasons why it is not likely that grain boundary diffusion (Fig. 4a and b) controls the local EBC. First, diffusion fields around garnet are not likely to be symmetrical, yet zoning profiles in garnet, and especially for MnO, are typically symmetrical. Second, it is far more likely that the small, high field strength elements such as Si and Al will diffuse more slowly than Mg, Fe, Mn or Ca through the grain boundaries. Indeed, Carlson (1991) has postulated that diffusion of Al may be rate-limiting in the growth of garnet and Spear and Daniel (2001) concluded that Si diffusion appears to be rate limiting for some samples.

Kinetic limitations on the release of nutrients by reacting matrix phases seems a more plausible explanation. Plagioclase is ubiquitously zoned in medium grade metamorphic rocks and shows extensive evidence in its chemical zoning for bulk dissolution and reprecipitation rather than homogenization by diffusion. The ease at which plagioclase can dissolve could, therefore, readily result in a lowered availability of CaO in epidote-free samples. Similarly, much of the MnO available for the production of spessartine component comes from ilmenite. Ilmenite has been identified as being refractory based on textural grounds (e.g. Hollister, 1969) and partitioning of MnO between ilmenite and garnet is rarely systematic, which argues again for the refractory nature of ilmenite. So it is possible that the lowered values of MnO in the EBC relative to the OBC is largely the result of the ilmenite dissolution kinetics.

For CaO in epidote-bearing samples, the results are somewhat less systematic. Two of the four samples show EBC CaO values to be higher than in the OBC whereas the other two show EBC CaO values lower than in the OBC. Assuming these results are correct and not a function of uncertainty in the Fe_2O_3 content, this could reflect kinetic controls on the dissolution of epidote or diffusive limitation of Ca to the growing garnet based on the proximity of reactant epidote crystals to the growing garnet.

4.1. Implications

The above results suggest that the EBC for the initial stages of garnet growth differs from the OBC owing to a number of factors that include the kinetics of mineral dissolution and intracrystalline diffusivity. Indeed, it is quite reasonable to extrapolate this conclusion to infer that the difference between the EBC and the OBC will continuously change as the phase assemblage changes, as phases grow (e.g. consider

fractionation of the bulk composition due to growth of garnet), the P and T change (which will have a first order effect on diffusivities), the amount and composition of fluid changes (which will affect mineral dissolution rates), and the strain history of the rock (which will impact the kinetics of reactant phase dissolution). Clearly, the fact that the EBC is substantially different from the OBC for these samples implies that equilibrium calculations such as pseudosections based on the OBC must be interpreted with caution, although they do provide the critical baseline for establishing the degree of overstepping. Approaches that do not rely on knowledge of the EBC, such as inclusion thermobarometry, will, fundamentally, be more robust so accurate estimations of the P-T conditions of metamorphism should pursue these approaches.

Acknowledgments

This study was supported by NSF grant 1447468 to Spear and the Edward P. Hamilton Endowed Chair fund. Thorough and insightful reviews by D. Waters and F. Gaidies greatly improved the presentation and are gratefully acknowledged.

References

- Carlson, W.D., 1991. Competitive diffusion-controlled growth of porphyroblasts. *Mineral. Mag.* 55, 317–330.
- Castro, A.E., Spear, F.S., 2016. Reaction overstepping and reevaluation of the peak P-T conditions of the Blueschist unit Sifnos, Greece: implications for the cyclades subduction zone. *Int. Geol. Rev.* 59, 548–562.
- Dragovic, B., Samanta, L.M., Baxter, E.F., Silverstone, J., 2012. Using garnet to constrain the duration and rate of water-releasing metamorphic reactions during subduction: an example from Sifnos, Greece. *Chem. Geol.* 314, 9–22.
- Gaidies, F., Pattison, D.R.M., de Capitani, C., 2011. Toward a quantitative model of metamorphic nucleation and growth. *Contrib. Mineral. Petrol.* 162 (5), 975–993.
- Gaidies, F., Petley-Ragan, A., Chakraborty, S., Dasgupta, S., Jones, P., 2015. Constraining the conditions of Barrovian metamorphism in Sikkim, India: P-T-t paths of garnet crystallization in the Lesser Himalayan Belt. *J. Metamorph. Geol.* 33, 23–44.
- George, F.R., Gaidies, F., 2017. Characterisation of a garnet population from the Sikkim Himalaya: insights into the rates and mechanisms of porphyroblast crystallisation. *Contrib. Mineral. Petrol.* 172.
- Hillert, M., 2008. *Phase Equilibria, Phase Diagrams and Phase Transformations: Their Thermodynamic Basis*. Cambridge University Press, Cambridge.
- Holland, T.J.B., Powell, R., 2011. An improved and extended internally consistent thermodynamic dataset for phases of petrological interest, involving a new equations of state for solids. *J. Metamorph. Geol.* 29, 333–383.
- Hollister, L.S., 1969. Contact metamorphism in the Kwoiek area of British Columbia: an end member of the metamorphic process. *Geol. Soc. Am. Bull.* 80, 2465–2494.
- Kohn, M.J., 2014. “Geob-Raman-try”: calibration of spectroscopic barometers for mineral inclusions. *Earth Planet. Sci. Lett.* 388, 187–196.
- Menard, T., Spear, F.S., 1994. Metamorphic P-T paths from calcic pelitic schists from the Stafford Dome, Vermont. *J. Metamorph. Geol.* 12, 811–826.
- Moynihan, D.P., Pattison, D.R.M., 2013. An automated method for the calculation of P-T paths from garnet zoning, with application to metapelitic schist from the Kootenay Arc, British Columbia, Canada. *J. Metamorph. Geol.* 31 (5), 525–548.
- Pattison, D.R.M., Tinkham, D.K., 2009. Interplay between equilibrium and kinetics in prograde metamorphism of pelites: an example from the Nelson aureole, British Columbia. *J. Metamorph. Geol.* 27, 249–279.
- Pattison, D.R.M., de Capitani, C., Gaidies, F., 2011. Petrological consequences of variations in metamorphic reaction affinity. *J. Metamorph. Geol.* 29 (9), 953–977.
- Prigogine, I., Defay, R., 1954. *Chemical Thermodynamics*. Longmans, Green and Co., London.

Spear, F.S., 2017. Garnet growth after overstepping. *Chem. Geol.* 466, 491–499.

Spear, F.S., Daniel, C.G., 2001. Diffusion control of garnet growth, Harpswell Neck, Maine, USA. *J. Metamorph. Geol.* 19, 179–195.

Spear, F.S., Pyle, J.M., 2010. Theoretical modeling of monazite growth in a low-Ca metapelite. *Chem. Geol.* 266, 218–230.

Spear, F.S., Selverstone, J., 1983. Quantitative P-T paths from zoned minerals: theory and tectonic applications. *Contrib. Mineral. Petrol.* 83, 348–357.

Spear, F.S., Thomas, J.B., Hallett, B.W., 2014. Overstepping the garnet isograd: a comparison of QuIG barometry and thermodynamic modeling. *Contrib. Mineral. Petrol.* 168 (3), 1–15.

St-Onge, M.R., 1987. Zoned poikiloblastic garnets: P-T paths and syn-metamorphic uplift through 30 km of structural depth, Wopmay Orogen, Canada. *J. Petrol.* 28, 1–22.

Thomas, J.B., Spear, F.S., 2018. Experimental study of quartz inclusions in garnet at pressures up to 3.0 GPa: evaluation of the quartz-in-garnet inclusion elastic thermobarometer. *Contrib. Mineral. Petrol.* 173 (42). <http://dx.doi.org/10.1007/s00410-018-1469-y>.

Thompson, C.V., Spaepen, F., 1983. Homogeneous crystal nucleation in binary metallic melts. *Acta Metall.* 31, 2021–2027.

Tomkins, H.S., Powell, R., Ellis, D.J., 2007. The pressure dependence of the zirconium-in-rutile thermometer. *J. Metamorph. Geol.* 25, 703–713.

Waters, D.J., Lovegrove, D.P., 2002. Assessing the extent of disequilibrium and overstepping of prograde metamorphic reactions in metapelites from the Bushveld complex aureole, South Africa. *J. Metamorph. Geol.* 20 (1), 135–149.

White, R.W., Powell, R., Holland, T.J.B., Johnson, T.E., Green, E.C.R., 2014a. New mineral activity-composition relations for thermodynamic calculations in metapelite systems. *J. Metamorph. Geol.* 32 (3), 261–286.

White, R.W., Powell, R., Johnson, T.E., 2014b. The effect of Mn on mineral stability in metapelites revisited: new a-x relations for manganese-bearing minerals. *J. Metamorph. Geol.* 32 (8), 809–828.

Wolfe, O.M., Spear, F.S., 2018. Determining the amount of overstepping required to nucleate garnet during Barrovian regional metamorphism, Connecticut Valley Synclinorium. *J. Metamorph. Geol.* 36, 79–94. <http://dx.doi.org/10.1111/jmg.12284>.